Abyssal Penetration and Bottom Reflection of Internal Tidal Energy in the Bay of Biscay

R. D. PINGREE

Plymouth Marine Laboratory, Citadel Hill, Plymouth, Devon U.K.

A. L. NEW

Institute of Oceanographic Sciences Deacon Laboratory, Brook Road, Wormley, Godalming, Surrey, U.K.

(Manuscript received 1 December 1989, in final form 18 June 1990)

ABSTRACT

This paper describes field observations in the Bay of Biscay, and presents convincing evidence for the existence of a broad beam of internal tidal energy propagating downward from a source region on the upper continental slopes, which, after penetrating the deep ocean interior along a theoretical ray path, reaches the abyssal plain, at a depth of about 4.2 km, 58 km from the source. The results concentrate on the region between 50 and 60 km from the generating area, where the beam of energy is below a depth of 2 km. A marked change in phase of the beam (4 hours) was observed over a distance of 12 km at a depth of about 3 km. In addition, semidiurnal currents were noticeably increased near the sea floor. These results are interpreted as demonstrating the occurrence of partial bottom reflection of the internal tidal energy, in agreement with theoretical predictions, at a distance of about 58 km from the generating region on the upper slope, and extend our previous results farther into the ocean.

1. Introduction

Large internal tides are generated by the interaction of surface tides with steep topography whenever the bottom slope matches the slope of the internal tidal characteristic (for example, see Gordon 1979; Baines 1982; Pingree and New 1989). Beams of internal tidal energy, characterized by large amplitude oscillations and relatively rapid changes of phase (in the vertical), are to be expected near ray paths emanating from these source regions. In the Bay of Biscay, the upper continental slope is critical in this sense at a depth of about 385 m (Pingree and New 1989). On theoretical grounds, three beams are expected, one beam over the shelf, initially propagating upward, and two in the oceanward, diminishes (Pingree and New 1989). The beams would be expected to reflect upon reaching ei- 1981; Baines 1982; New 1987). With more rounded upperslope topography, the upward beam, propagating oceanward, diminishes (Pingree and New 1989). The beams would be expected to reflect upon reaching either the sea surface or the sea bed and, theoretically, the phase along the centerlines of the beams would be expected to be constant, except where such reflections occurred.

The existence of beams of internal wave energy propagating along characteristic ray paths has been demonstrated in the laboratory by Mowbray and Rarity (1967), by using a mechanically oscillated source (see also Turner 1973). However, their detection in nature has been difficult, possibly because of dissipation by wave–wave interactions, mixing and internal friction as the energy propagates away from the generation region (Schott 1977). Larsen et al. (1972) were, perhaps, the first to attempt to find these rays in nature, but their observations (off Vancouver Island) were contaminated with ship motions and so no results were presented. Barbee et al. (1975) then went on to deploy a single mooring in the same location and managed to detect a maximum in the oscillation amplitudes near the expected position of the ray. Unfortunately, the amplitudes were 3–4 times larger than those predicted by a numerical model, and there were phase discrepancies of, on the average, almost 180°, so that the results were open to question. Recently, however, Pingree and New (1989, subsequently referred to as PN), by deploying moorings and making a series of semidiurnal-period CTD stations on a line perpendicular to the shelf break at about 47°30′N in the Bay of Biscay, were able to convincingly demonstrate the existence of a distinct beam of tidal energy propagating along a theoretical ray path. To our knowledge, this is the first demonstration of such a phenomenon in nature. These observations were made to 37.5 km from the generation region, and stopped short of the predicted bottom reflection, but clearly showed a beam of internal tidal energy traveling downward into the deep ocean. Large amplitudes were observed in the beam at every station,

Corresponding author address: Dr. Robin Pingree, Plymouth Marine Laboratory, Citadel Hill, Plymouth, Devon PL1 2PB, United Kingdom.

ranging from approximately 150 m near the upper slopes to 100 m farther out, and, in particular, both amplitudes and phases of the observations were well represented by the numerical model of New (1988). This provided confidence in both the model and in the interpretation of the observations. One likely reason for the success of this experiment was the strength of the signal [for instance Barbee et al. (1975) only found maximum amplitudes of less than 20 m]. Indeed, Baines (1982) has indicated that the shelf break in the Bay of Biscay between 47° and 49°N may be responsible for the production of some of the most energetic internal tides anywhere in the world.

This paper describes results obtained from a cruise made by the RRS *Challenger* in the Bay of Biscay between 27 June and 15 July 1988, but some comparisons are also made with data collected during a cruise in September 1987. The propagation of internal tidal energy from the upper slopes is followed downward to the Biscay abyssal plains, to greater distances than was achieved by PN. A theoretical beam of internal tidal energy, starting from a source on the upper slopes and following a calculated ray path (at the M_2 tidal frequency), is predicted to reflect off the sea floor at a depth of 4.2 km and at a distance of 58 km from the critical zone. The results presented here concentrate on the region between 50 and 60 km from the source, where the beam of energy is below 2 km in depth and bottom reflection is anticipated. As such, these observations extend the results of PN and provide an investigation of the bottom reflection of the beam of internal energy. In addition, some results from slope current meter moorings of earlier years (1984, 1985) have been used to relate the internal tidal oscillations on the upper slopes to the conditions that were found at a mooring positioned near the point of bottom reflection.

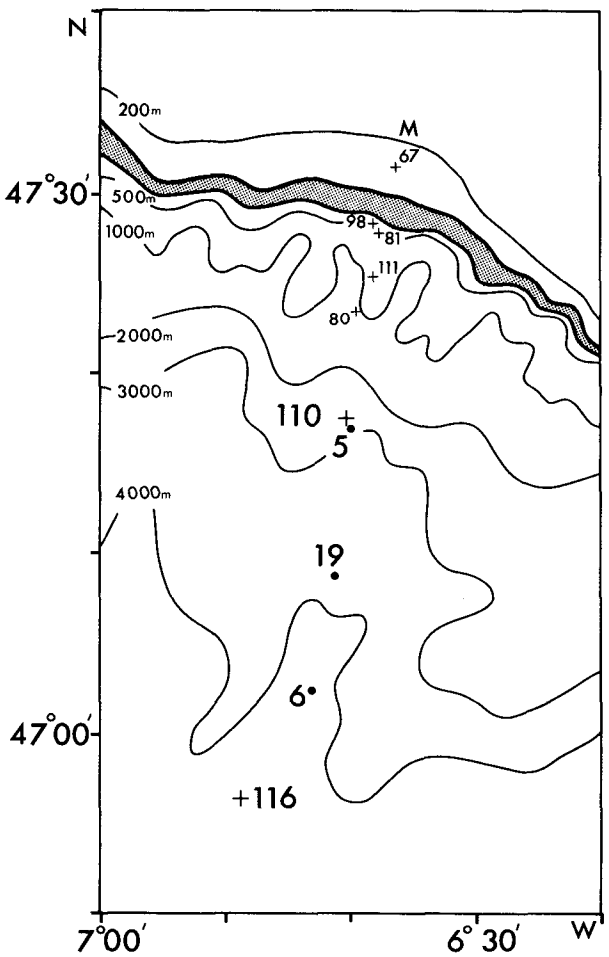

FIG. 1. Positions of mooring 116 and tidal period CTD stations 5 and 6 (*Challenger*, July 1988). Also shown are positions of moorings 110 and tidal period CTD station 19 (*Challenger*, September 1987). The critical depth on the upper slopes occurs at about 385 m, and depth contours between 300 and 400 m are shown shaded. Also shown are the positions of the upper slope moorings (67, 98, 81, 111, 80) that have been used to determine the semidiurnal internal tidal amplitudes and phases near the generation region (see Table 2). The tidal characteristics at point M derived from a barotropic model are also defined in Table 2.

Pingree and New found that, in the Bay of Biscay, the beam of internal tidal energy was at least 1 km wide at a depth of 2 km. The results presented here show that, near the theoretical point of bottom reflection, the "beam," or zone of increased isotherm oscillations, covers just over the lower half of the water column, (i.e., from 1600 to 4200 m depth). In addition, large near bottom currents, and a marked change of phase in the internal tidal beam, were observed near the predicted position of the bottom reflection; both facts indicate that the beam has at least partially reflected by about 60 km from the generating region. Observations farther from the slope are expected to show a more complete reflection. However, we believe this is the first time that comprehensive field observations have been made of internal tides penetrating to, and, in particular, reflecting from, abyssal depths.

2. Results from CTD stations and thermistor chain moorings

On *Challenger* Cruise 31/88 (27 June to 15 July 1988) a deep mooring (116) was deployed in a water depth of 4202 m, near the point of bottom reflection for a beam of internal tidal energy emanating from the upper slope (Fig. 1). Two CTD stations were also undertaken. The first, CTD5, was conducted on the slopes in a water depth of 3056 m and at a distance of 22 km from the critical depth contour (Fig. 1). This position was chosen to coincide as nearly as possible with the position of mooring 110 (deployed in 1987 and used by PN) in order to establish whether conditions in July 1988 were similar to those experienced by PN in September 1987. The second CTD station, CTD6, was performed at 49 km from the critical slope in order to extend the results of PN to a position where the pre-

dicted beam of internal tidal energy (New 1988) and calculated ray path were at a depth of 3 km.

The CTD stations were tidal yoyo stations. Each station was occupied for one semidiurnal tidal period near spring tides, while the CTD was continuously raised and lowered at a speed of 1 m s^{-1}. Profiles were made from the surface to within about 20 m of the bottom while RRS *Challenger* maintained a fixed position relative to a dahn buoy anchored to the bottom. The isopycnals were referenced to the 0, 1000 and 2000 db levels, for the purpose of estimating the amplitudes and phases of the internal tidal oscillations throughout the water column. At pressures approaching 3000 db and deeper, it was found more convenient to use potential temperature rather than isopycnal displacements as the theoretical advantages of using isopycnal surfaces at these depths can be offset by the practical difficulties of determining salinity with sufficient resolution. At 3000 db in this region the potential temperature gradient is typically 0.06°C per 100 db whereas the salinity gradient is about 0.004‰ per 100 db. Salinity noise levels were generally within 0.001‰ but spurious salinity jumps of up to 0.002‰ occurred below 3000 db. By contrast, temperature was relatively very stable with a resolution of about 0.001°C. At pressures greater than 3500 db, the gradients of potential temperature and salinity are even further reduced and using the salinity data to calculate the isopycnals resulted in a reduced ability to resolve the amplitude of the internal tidal oscillations.

From the tidal-period CTD stations and thermistor chain/current meter mooring, the semidiurnal amplitudes and phases of the internal tide were estimated from the positions of the crests and troughs of various isopycnals (or isotherms) in the manner described by

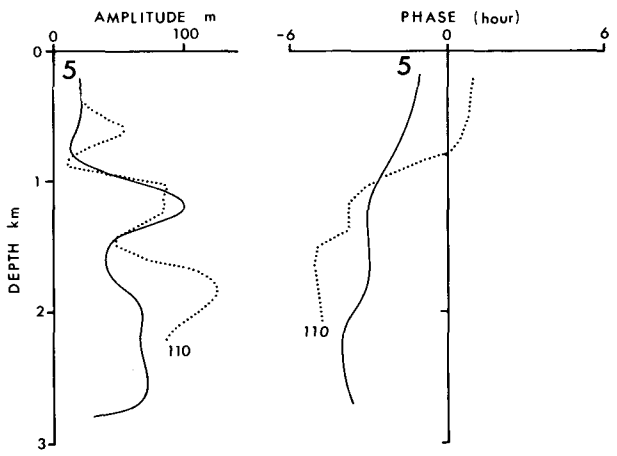

FIG. 2. Profiles of amplitude and phase with respect to high water Plymouth (HWP) at CTD tidal yoyo station 5 (from 0120 UTC to 1750 UTC, 1 July 1988) in a water depth of 3056 m. Also shown (dotted) are profiles of amplitude and phase at the nearby mooring site 110 (obtained by Fourier analysis of 4 semidiurnal periods starting at HWP (1833 UTC) on 8 September 1987).

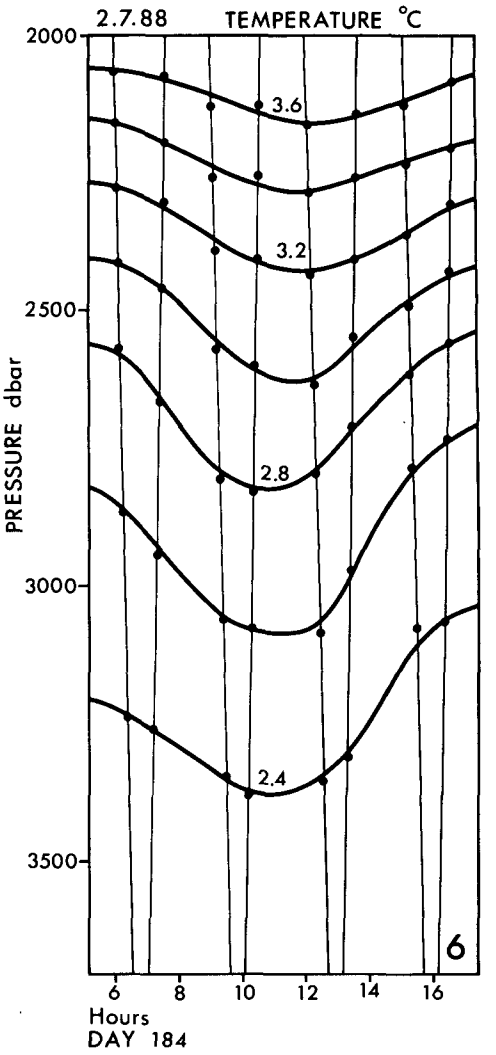

FIG. 3. Isotherms of potential temperature against time (starting at 0510 UTC 2 July 1988) obtained at tidal yoyo station 6 (whilst maintaining position on a dahn anchored to the sea floor in a water depth of 4126 m), illustrating the large amplitude oscillations (about 300 m peak to trough) found at depths of about 3000 m. The near vertical lines represent the path of the CTD through the water column and the isotherms have been drawn by eye through the spot values (dots) of selected potential isotherms. HWP is at 0744 UTC.

PN. This operation was performed for each station and throughout the water column, and the results were plotted at the mean depth of the chosen isopycnal. In this manner a depth profile for each station was constructed of the amplitude, η', (equal to one-half peak-to-trough displacement) and phase, θ, (the time in hours after high water at Plymouth (HWP) of the local maximum upward displacement) of the internal tidal displacement η, where for each station,

$$\eta = \eta'(z) \cos \frac{2\pi}{T} (t - \theta(z)) \qquad (1)$$

where T is the semidiurnal tidal period and t is the time in hours after HWP.

a. Amplitude and phase profiles at CTD5 and CTD6

At CTD5, the amplitudes and phases of the internal tidal oscillations were estimated from ten profiles (Fig. 2). Maximum amplitudes were found at a depth of about 1200 m where the peak to trough oscillations increased to 200 m. This maximum is identified as the main beam of internal tidal energy emanating from the upper slopes and is practically coincident with the beam found by PN near the same position (their Fig. 11) from an analysis of the results of mooring 110 (which had 71 thermistors spaced throughout the water column). There was also some evidence for locally increased amplitudes in the deeper part of the water column. At mooring 110 these increased oscillations (i.e., below 1500 m) were composed of almost equal contributions from the M_2 and S_2 tidal constituents. No further light on the source of this disturbance was found (or sought) in the present study.

At CTD6, in a water depth of 4126 m, the amplitudes and phases of the internal tidal oscillations were estimated from eight profiles. Maximum amplitude oscillations of potential temperature were found, as anticipated, at a depth near 3 km with peak-to-trough oscillations approaching 300 m (Fig. 3). The complete amplitude and phase profile obtained at CTD6 shows the internal tide effectively absent from the upper 2 km of the water column (Fig. 4). For comparison the amplitude and phase profile derived at CTD19 (the farthest offshelf station in PN), which was about 11 km nearer the slope (see Fig. 1 for station position) is also shown. Maximum amplitudes occurred at about 2 km depth and CTD19 also revealed little evidence of internal tidal activity in the upper part (<1 km) of the water column. The downward trend, between these two stations and CTD5, of internal tidal energy to abyssal depths is quite apparent.

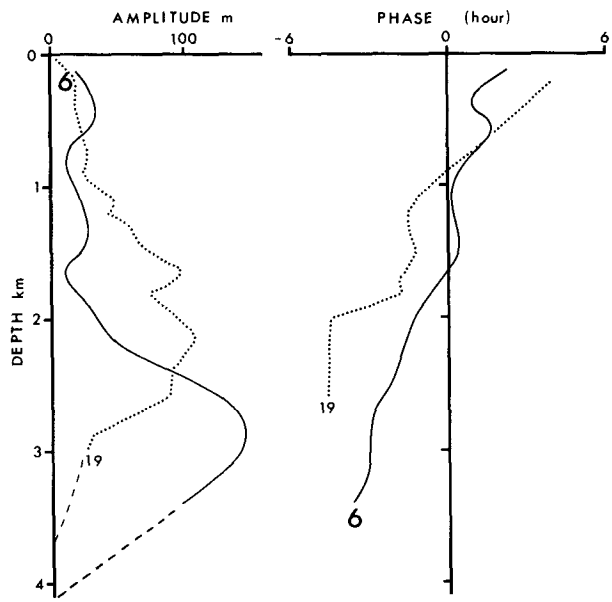

FIG. 4. Estimated profiles of amplitude and phase at CTD station 6 during the period from 0510 to 1720 UTC 2 July 1988. Also shown (dotted) are profiles of amplitude and phase determined at CTD station 19 (0900 to 2200 UTC, 23 September 1987). Dashed lines are interpolated values assuming that the amplitude falls to zero at the sea floor (see for example Fig. 8).

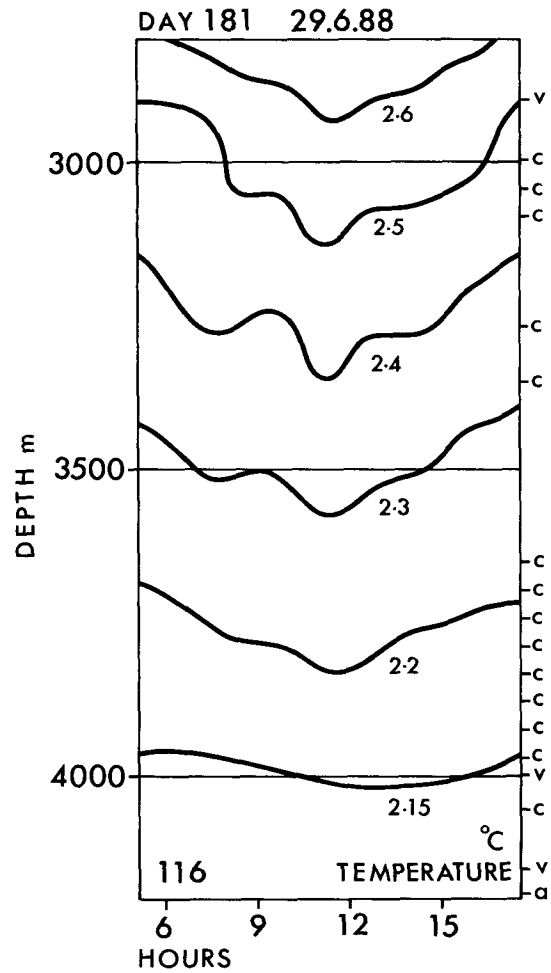

FIG. 5. Isotherms of potential temperature against time after HWP (HWP is at 0512 UTC) obtained at mooring 116 on 29 June 1988, showing large oscillations (about 250 m peak to trough) at a depth of about 3000 m in a water depth of 4202 m. These contours have been corrected for mooring motion and the undisturbed depths of the thermistors are given by the positions marked at the right hand side of the figure. The instruments on the mooring are identified by 'v' (VACM), 'c' (thermistor chain) and 'a' (Aanderaa current meter).

b. Mooring 116

1) ISOTHERMS

Higher time resolution (5 min sampling) of potential temperature illustrating the character of the internal tidal oscillations was obtained from mooring 116,

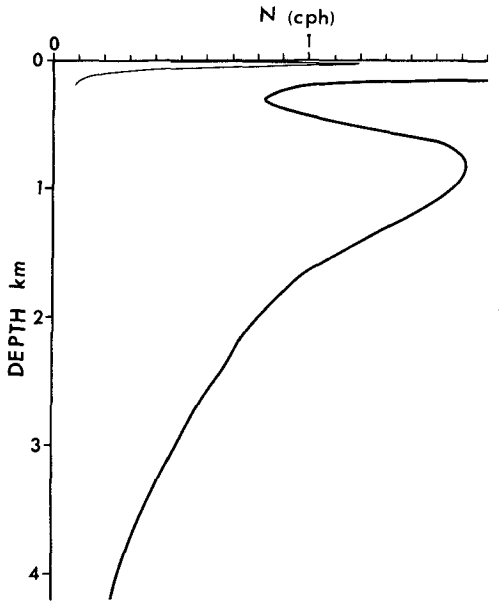

FIG. 6. Brunt-Väisälä frequency in cycles per hour against depth in km for the central region (near 47°N, 6°45'W) of the Bay of Biscay. The results above 200 m (thin line) apply to the developing thermocline at CTD6 and for this region the unit on the abscissa scale should be multiplied by 10.

which was deployed for 10 days (28 June to 9 July 1988) at 46°56.5'N, 06°49.0'W, 62 km from the critical depth on the upper slopes. While moorings may give increased time resolution compared with deep tidal yoyo CTDs, the results are nevertheless limited by the number of recording instruments that operate successfully during the period of the mooring deployment. The instrumentation on mooring 116 covered the water column from 812 to 4195 m. Some loss of data coverage occurred in the depth range between 2900 to 3600 m when, after 20 hours of deployment, the thermistor logger spanning this region flooded.

Temperature oscillations in the bottom 1.4 km covering a complete tidal cycle (before loss of data occurred) exhibited peak-to-trough displacements of about 200 m at depths of about 3 km (Fig. 5). Also evident are higher period oscillations close to the Brunt-Väisälä period, which at 3600 m is 3 h (Fig. 6). Averaging eight tidal cycles centered near spring tides, for all thermistor records which gave high quality data throughout the complete period of the mooring deployment, resulted in a smoothed plot of the potential temperature isotherms (Fig. 7). Oscillations reached maximum peak-to-trough amplitudes of about 200 m at a depth of 3 km. Equally noticeable is the absence of a discernable tidal oscillation at depths above about 1600 m during this spring tide period. The amplitude and phase profiles for these observations (Fig. 8) were obtained manually (as in PN) and by Fourier analysis for the semidiurnal component of an isotherm displacement (corrected for mooring motion). Similar estimates were obtained using the mean potential temperature gradient determined at CTD6 rather than interpolating for the displacement of an isotherm between thermistors. Relatively large quarter diurnal effects were noted at mooring 116 at about 1900 m (0.46 of the

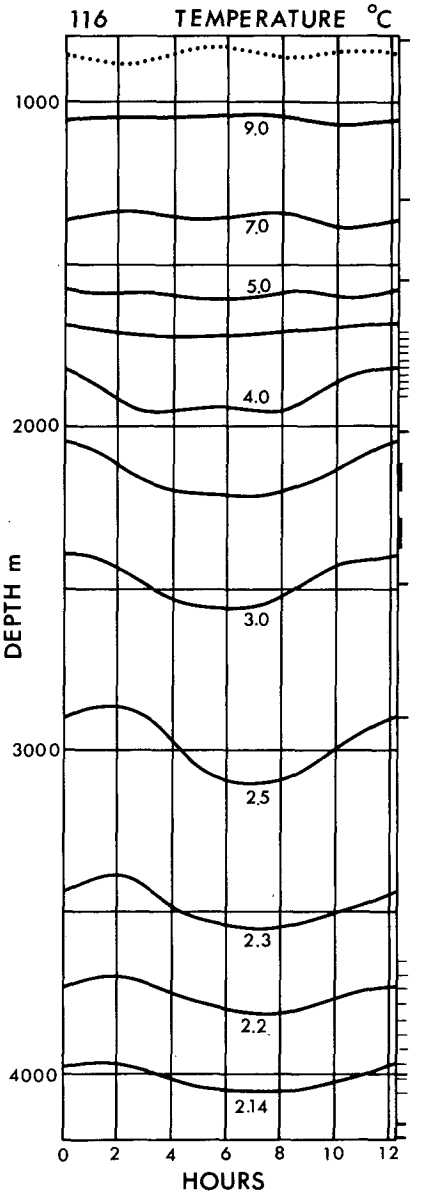

FIG. 7. Isotherms of potential temperature obtained from the instrumentation on mooring 116 (in a water depth of 4202 m) against time in hours after HWP. Eight consecutive semidiurnal tidal cycles have been averaged starting at 2000 UTC 2 July 1988 (Day 184). These interpolated contours have been corrected for mooring motion and the undisturbed depths of the thermistors are given by the positions marked at the right-hand side of the figure. The two bold lines are 75 m thermistor chains with 11 sensors on each chain. The undisturbed depth of the top thermistor is 812 m; its actual depth, as determined by a pressure sensor, is shown by the dotted contour.

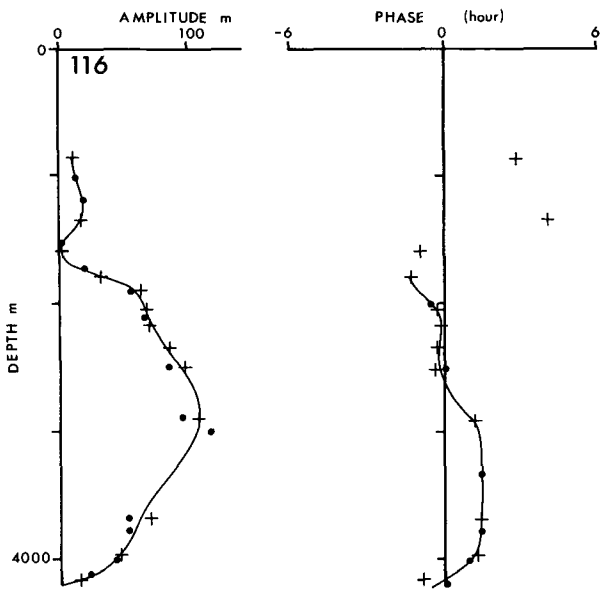

FIG. 8. Profiles of amplitude and phase obtained at mooring 116 for the mean spring tide conditions illustrated in Fig. 7. Dots are estimates (as in PN) and crosses are values determined by Fourier analysis for the semidiurnal frequency.

semidiurnal amplitude) and near the bottom (0.31 of the semidiurnal amplitude); in both cases the phase was such as to give peaked crests and flattened troughs (as illustrated by the 4°C potential temperature isotherm of Fig. 7). The semidiurnal results (Fig. 8) demonstrate, as before (CTD6, Fig. 4), that the oscillations are largely confined to the lower half of the water column. However, the phases in the lower part of the water column (between 3 and 4 km depth) are in marked contrast to those found at CTD6, being about 4½ hours delayed. This marked change of phase, occurring in little more than a distance of 10 km, taken together with the fact that the largest oscillations occur at depth, is interpreted as demonstrating partial bottom reflection of a broad beam of internal tidal energy that has penetrated to the Bay of Biscay abyssal plain. Note also that the phase delay (Fig. 8, mooring 116) with increasing depth from 2 to 3 km is in marked contrast to all other profiles, which show an advance of phase on passing downward through the beam. This change of phase with depth is consistent with an upward-propagating beam of energy at mooring 116 (see below).

2) CURRENTS

Further evidence for abyssal penetration of internal tidal energy is provided by the current meter records on mooring 116. Maximum semidiurnal near bottom currents reached 16 cm s^{-1} near spring tides, considerably in excess of barotropic values (about 2 cm s^{-1}). Table 1 gives a least squares analysis for the M_2 and S_2 tidal components in terms of their ellipse properties. The vertically integrated or barotropic estimate is polarized in an anticlockwise sense. This is consistent with a predominantly Kelvin wavelike motion that forces a cooscillation in the Bay of Biscay as it propagates northwards in the NE Atlantic. The baroclinic M_2 and S_2 components, obtained by subtracting the barotropic estimates from the individual records, are generally polarized in a clockwise sense, though less than expected for progressive modes coming from a single direction (ratio of semiminor to semimajor axes, $b/a = f/\sigma \sim 0.76$). However, the M_2 currents have increased values near the bottom at 4 km depth and this is consistent with bottom reflection [i.e., numerical models show that the beams of energy are also associated with anomalously large currents (e.g., New 1987]. Furthermore, the ellipse direction (~018°, 203 m off bottom) is also close to the direction from which the internal tidal energy is assumed to be propagating. Short records in the presence of noisy signals do not

TABLE 1. Tidal analysis of the barotropic and baroclinic current at mooring 116 in a water depth of 4202 m (46°56.5'N, 06°49.0'W) over the period 28 June to 9 July 1988.

	M_2				S_2			
Depth of current meter (m)	Amplitude a (cm s^{-1})	b/a (%)	Phase (°g)	Orientation (°T)	Amplitude a cm s^{-1}	b/a (%)	Phase (°g)	Orientation (°T)
812	6.0	49c	176	034	4.8	86c	334	158
1544	2.8	42c	184	001	5.9	60c	191	049
2017	6.1	66c	143	001	3.5	51c	105	148
2482	2.2	9c	027	168	3.1	71c	111	155
2896	3.1	61c	325	027	6.6	72c	039	043
3999	10.4	60c	358	018	1.8	35c	010	013
4195	10.4	35c	003	019	1.7	10a	330	040
Barotropic estimate	1.8	78a	324	150	1.1	13c	117	014

c: clockwise.
a: anticlockwise.

allow us to say much about the S_2 component. It is probable that the increased value of the S_2 currents at 3 km depth indicates a more complete reflection of the higher frequency S_2 component. Clearly, longer records are required.

3. Propagation of internal tidal energy to the abyssal plain

Ray slopes, c, are given by

$$c^2 = \frac{\sigma^2 - f^2}{N^2 - \sigma^2} \tag{2}$$

where σ is the semidiurnal tidal frequency ($\sigma = 1.405 \times 10^{-4}$ s^{-1} for the M_2 principal component), f is the Coriolis parameter ($f = 1.070 \times 10^{-4}$ s^{-1} at 47°10′N) and N is the Brunt-Väisälä frequency.

The results of this study, extending our earlier work in September 1987 (PN), are summarized in Fig. 9. The ray path shown emanating from the critical region on the upper slopes and reflecting off the bottom was determined using Eq. (2), in which the mean stability frequency, N, had been accurately determined by averaging all the deep tidal yoyo CTD stations from the 1987 and 1988 studies (Fig. 6). The depths of the maximum oscillation found at each station fall close to a ray path which has a local slope given by (2), and reflects from the sea bed. The observed beam is broad, and even when defined by 70% generators (i.e., depths where the amplitude falls to only 70% of the maximum

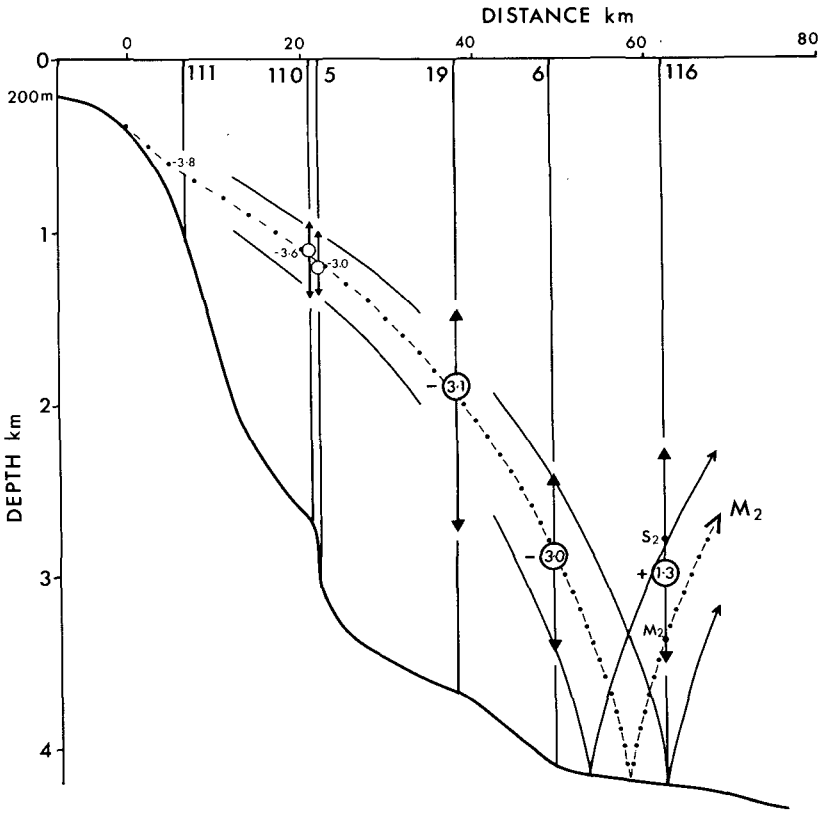

FIG. 9. Diagram showing the theoretical ray path (chained line) for a beam of internal tidal energy at the M_2 tidal frequency emanating from the critical depth (385 m) on the upper slopes and reflecting off the Biscay abyssal plain at a depth of about 4200 m, 58 km from the critical point. Also shown is a summary of the internal tidal oscillations obtained during the RRS *Challenger* cruises in 1988 (CH 31/88) and 1987 (CH 18/87). Vertical lines represent mooring and CTD station positions and are identified with numbers. CTD stations 5 and 6 and mooring 116 are from the 1988 cruise, whereas moorings 110 and 111 and CTD 19 were obtained in 1987. The depth of the maximum amplitude of the internal tidal oscillation found at each station is plotted as an open circle and the range where the amplitude is more than 70% of the maximum value is indicated by the arrows. Two further rays are shown (solid lines) passing through the 70% limits near mooring 110. The phase of the maximum upward displacement is given (within the circles) in hours with respect to HWP. A ray at the M_2 tidal frequency would intersect mooring 116 at the depth marked M_2; S_2 is the corresponding point for a ray at the S_2 tidal frequency. The topography is depicted by the bold line and is critical at 385 m; the horizontal distance scale is measured from the critical point.

oscillation) it is still more than 1 km in vertical extent where it reaches abyssal depths. The mean phase of the maximum upward displacement on the downward path of the beam is 3.3 h before HWP, but at mooring 116 a phase delay of about 4½ h is in evidence, resulting in a phase of 1.3 h after HWP, and indicating partial bottom reflection, as described below.

The numerical model of New (1988) was applied as described in PN, for a spring tide condition, and the results are shown in Figs. 10a and 10b as contour plots of the internal tidal oscillation amplitudes (m) and phases (hours after HWP), near the initially downward-propagating main beam. The amplitudes are largest near the theoretical ray path, and generally increase as the ray descends (due to the decreasing stratification), except near the point of bottom reflection (where the amplitude must reduce to zero). These amplitudes are qualitatively in good agreement with those found in the CTD stations and moorings, and differences most probably result from the lack of dissipation in the model as the beam propagates from the generating region. The predicted phases are shown in Fig. 10b and reveal that the downward ray (before bottom reflection) is associated with a constant phase of about 3.2 h before HWP, with a phase lag above the beam, and a phase lead below. The predicted phase down the ray is in excellent agreement with the observations (3.0 to 3.8 h before HWP, Fig. 9), as is, qualitatively, the phase advance with increasing depth through the beam (Figs. 2 and 4). Far enough after reflection from the bottom bounce (e.g., 80 km or more from the generation site), the phase along the ray is again constant and predicted to be 3.0 h after HWP (i.e., a change of precisely +180°). However, immediately after the predicted bounce (e.g., at 62 km for mooring 116), the phase is approximately 2.3 h after HWP, in good agreement with the observed value (1.3 h after HWP). In addition, the oscillations above the ray are now in advance of those below it, and this phase lag with increasing depth also agrees qualitatively with the observations (Fig. 8). From the model, we see that the ray cannot be considered to have fully reflected before about 80 km from the upper slopes. For instance, farther out than this position, the phase along the ray becomes constant and the amplitude contours (>50 m) in the beam are confined to a relatively thin pencil, of about the same thickness as the incident ray; closer to the predicted bottom bounce (60 to 80 km), the phase along the ray is not constant and the region of large amplitudes is of increased vertical extent, so that the incident and reflected beams are considered to be overlapping. Consequently, the observations at mooring 116 (62 km), well represented by the model, and showing a +4 to +5 hour phase change as compared with the incident ray, are considered as providing firm evidence of a partial bottom reflection of the internal tidal beam of energy (i.e., moorings further than about 80 km from the upper slopes are expected to show the full +6.2 hour phase change). We believe these are the first observations of the occurrence of such a phenomenon.

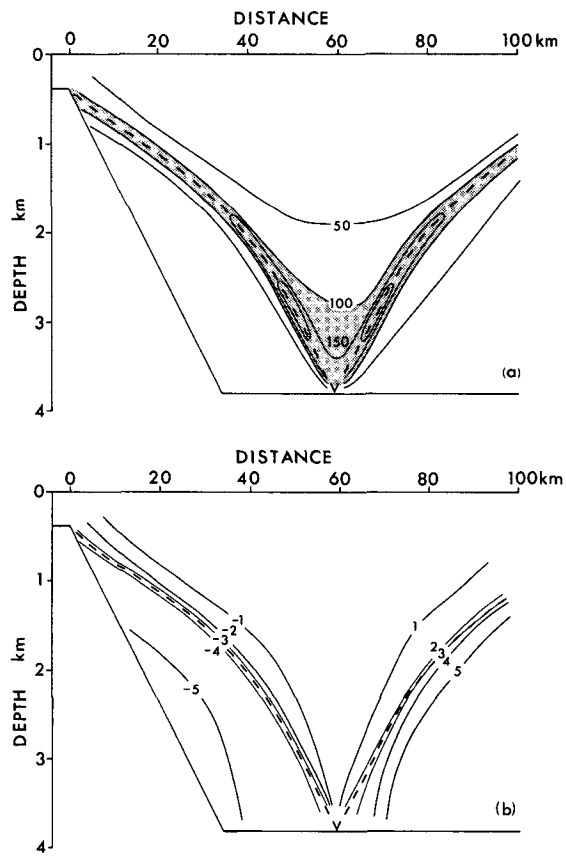

FIG. 10. Numerical model (see New 1988) (a) amplitudes, η' (meters), and (b) phases, θ (hours after HWP), near the main, initially downward-propagating ray path (broken line). The model topography consists of a shelf depth of 385 m and an ocean of 3800 m, connected by a linear slope of 0.1, as indicated. Horizontal distance is measured from the critical point (in this case the shelf break), and the phases were calculated by assuming that maximum off-shelf tidal streaming occurred at 2 h after HWP (g_{M_2} for Plymouth ~ 154°, see also Table 2).

4. Modes

Any description of the internal tidal oscillations in terms of rays has an equivalent in terms of modes though the physical insight gained in such a description may not be so enlightening, particularly over a sloping bottom. At mooring 116, the mean bottom slope is nearly flat with a ratio of bottom slope to ray slope of order 0.1. The phases of the baroclinic M_2 currents near the bottom (358°, 003°, Table 1) are approximately 180° out of phase with the phase of the maximum internal tidal oscillations (171°, see Table 2 for an M_2 analysis of the 2.52°C potential temperature isotherm in the beam), implying a progressive wavelike character (propagating from a direction of 019°, Table

1) for the internal tide, and it is instructive to see whether the observations can be represented by a single dominant free mode.

The first 5 modes were calculated from the Taylor-Goldstein equation

$$\frac{d^2\eta'}{dz^2} + k^2 \frac{(N^2(z) - \sigma^2)}{(\sigma^2 - f^2)} \eta' = 0 \qquad (3)$$

(where $\eta'(z)$ is the amplitude of a mode), using the data from CTD6 to determine $N(z)$ in the upper 200 m (Fig. 6), and are presented in Fig. 11. The amplitudes of the isotherm displacements are of course arbitrary, but for illustrative purposes each has been plotted on a scale such that the M_2 amplitude at the beam depth for mooring 116 (2900 m) corresponds with the observations (80 m, Table 2). The associated bottom currents for each mode are listed in Table 3, for which the horizontal currents, u, associated with each modal amplitude, η', were calculated from the relationship

$$u = \frac{\sigma}{k} \frac{d\eta'}{dz}. \qquad (4)$$

Modes 1, 2 and 3 are little affected by the presence of the seasonal thermocline, though with a more developed late summer thermocline mode 3 is significantly turned in the upper 100 m and becomes dominant here (Pingree et al. 1986; New 1987). While it is seen that mode 2 has the closest fit to the observed bottom currents (Table 1), it has a zero crossing at a depth of 1260 m and so contributions from further modes are required to result in the observed near zero displacement of isotherms at a depth of 1600 m (Fig. 8). No simple picture emerged from a least squares modal fit to the data, though modes 2 and 3 tended to be dominant at 3 km depth.

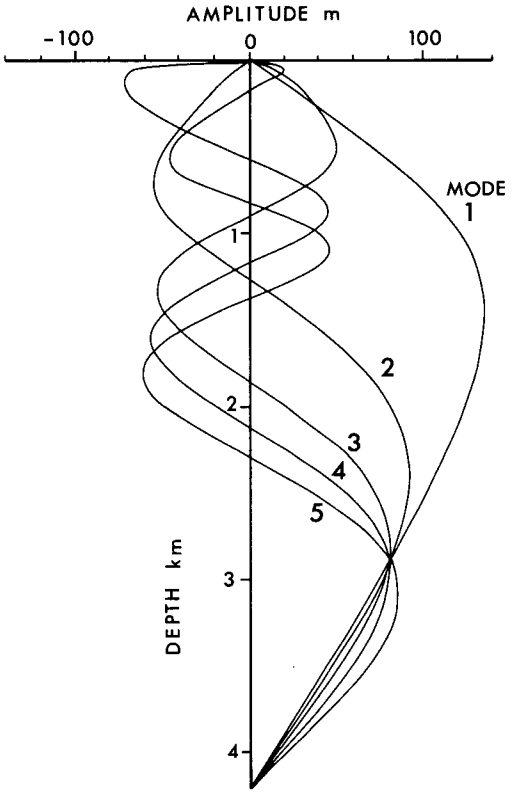

FIG. 11. First five M_2 baroclinic modes calculated for the Brunt-Väisälä frequency profile shown in Fig. 6.

5. Comparison between upper slope moorings and mooring 116

A comparison between mooring data and CTD data over a tidal period, during spring tide conditions, has allowed the propagation of a broad beam of internal tidal energy to be followed, and has established continuity of the beam from the upper slopes to the abyssal plains. The more extended datasets from moorings deployed on previous cruises (numbers 067, 080, 081, 098, 110, 111, see Fig. 1) allow us to tie in the phases of the internal tidal oscillations on the upper slopes with the observations at mooring 116, near the point of reflection, more accurately. The results from these moorings have been analyzed into their M_2 and S_2 tidal constituents and are summarized in Table 2. It should be pointed out however that the internal tidal amplitudes and phases are not strictly M_2 and S_2 tidal components since the data were gathered over the summer and autumn periods and there is no guarantee that similar conditions will prevail during the winter and spring periods. Indeed, PN showed that winter mixing at the shelf break could increase the depth of the critical slope, so that some differences between summer and winter conditions are anticipated.

We start by defining the barotropic tidal currents on the upper slopes, which effectively drive the baroclinic internal tides. The barotropic tidal currents derived from a numerical model (Pingree et al. 1984) show that, at the shelf break in this region, the tidal ellipses are rotary clockwise with semi-major axes that are approximately normal to the shelf break (Table 2). The ratio of the S_2/M_2 amplitude is about 38%. The phase difference between the S_2 and M_2 components is 41°, and this difference gives the phase lag of spring tides after new or full moon. [The age of the tide expressed in hours (i.e., 40 h) is nearly equal to (~0.98×) the phase difference (41°) expressed in degrees.] Similar results were obtained from measurements at mooring 067 near the shelf break (Fig. 1). From the shelf break to depths of 500 m (see the results from moorings 081 and 098, where the data from seven current meters were summed vectorially), the M_2 currents decrease from about 50 to about 20 cm s^{-1}, largely due to the effects of continuity. A decrease in the ellipticity (b/a) of the tidal ellipses also occurs since the ellipses become polarized in an anticlockwise sense in deeper water (Table 1) both as a result of the reflection of the

TABLE 2. Tidal analysis of barotropic currents and of the displacement of selected isotherms at increasing distances from the upper slopes.

Mooring number Position Water depth Record length (days)	Temperature of selected isotherm (mean depth of isotherm)	M_2				S_2				S_2/M_2 (%)	Age $g_{S_2} - g_{m_2}$	Distance from the critical contour (385 m) (km)
		Amplitude a (cm s^{-1}) m	b/a (%)	Phase (°g)	Orientation (°T)	Amplitude a (cm s^{-1}) m	b/a (%)	Phase (°g)	Orientation (°T)			
M Barotropic Model 200 m	—	(46)	(60c)*	(044)	(026)	(17)	(58c)	(085)	(026)	(38)	(41)	—
067 (2)+ 47°31.7'N 06°36.7'W 206 m (25)	—	(51.5)	(62c)	(038)	(026)	(15.5)	(68c)	(080)	(027)	(30)	(42)	—
081 (4)+ 098 (3)+ 47°28.2'N 06°38.3'W 524 m	—	(19.3)	(39c)	(030)	(030)	(8.1)	(50c)	(073)	(032)	(42)	(43)	
(90) (64)	11.3°C (316 m)	85	—	062	—	48	—	112	—	57	50	2
111 47°25.3'N 06°38.3'W 1101 m (18)	10.00°C (821 m)	45	—	025	—	34	—	075	—	75	50	7
080 47°23.4'N 06°39.6'W 1503 m (90)	9.75°C (775 m)	52	—	047	—	42	—	085	—	81	41	11
110 47°17.6'N 06°40.3'W 2639 m (16)	9.39°C (1104 m)	50	—	051	—	27	—	103	—	54	52	21
116 46°56.5'N 06°49.0'W 4202 m (10)	2.52°C† (2941 m)	83	—	171	—	38	—	283	—	46	111	62

* c denotes clockwise rotation.
+ Number of current meters used in the estimate.
† Potential temperature.

TABLE 3. Modes for Biscay stratification.

Mode	Wavenumber κ (km^{-1})	Phase speed σ/κ ($m\ s^{-1}$)	Bottom currents based on M_2 amplitude of 80 m at 2900 m depth ($cm\ s^{-1}$)
1	0.04	3.5	22
2	0.09	1.5	10
3	0.14	1.0	8
4	0.17	0.8	7
5	0.20	0.7	7

Kelvin wave in the Bay of Biscay and the Poincaré wavelike motion on the Armorican shelf (Le Cann 1990). Maximum upslope barotropic tidal streaming in the internal tide generation zone (at a depth of 385 m) occurs at 034°g (mean of moorings 067 and 081, Table 2) for the M_2 tide (or perhaps a few degrees earlier, since the normal slope direction is about 015°T, whereas the barotropic ellipses are aligned at more nearly 028°T).

Also presented in Table 2 are the results of tidal analyses of the displacement of selected isotherms from the upper slope moorings. These have been chosen such that the mean depth of the selected isotherm coincided as closely as possible with the depth of the M_2 ray path (Fig. 9) at the mooring position, but with the restriction that the isotherm had to be contained within the span of the instrumentation on the mooring throughout the period of the tidal analysis. At mooring 111, the mean depth (821 m) of the selected isotherm (10.0°C) is somewhat deep because this mooring did not span the upper part of the water column. At moorings 081 and 098 the selected isotherm is rather shallow since the isotherm representing the main beam descended to depths greater than the water depth at this mooring position. To distances of 20 km from the critical slope, the mean amplitude of the M_2 component is 58 m, with a further contribution of 38 m from the S_2 tide, resulting in peak to trough oscillations of nearly 200 m at spring tides. The S_2/M_2 amplitude ratio is high (~66%, mean of 081, 098 and 111), suggesting preferential generation of the S_2 tide, perhaps due to favorable topography and stratification. The average phase of the M_2 internal tide (to 21 km from the critical slope) is 046°g, which shows that the maximum upward displacement of the isotherms along the beam lags the maximum upslope tidal streaming in the generation region by about ½ h. Maximum internal tides occur about 5 h (age of internal tide minus age of barotropic tide) after barotropic spring tides on the upper slopes.

The CTD tidal yoyo stations indicate that these conditions of reasonably constant phase, along the M_2 ray path, hold to distances of 50 km from the critical slope. However, the results from mooring 116, a further 12 km oceanward, show a marked increase in phase for the M_2 internal oscillation of the 2.52°C potential temperature isotherm (which has a mean depth of 2941 m and corresponds with the depth of the maximum in the amplitude profile, Fig. 8). This phase lag is equivalent to 4.3 h (171°g − 46°g = 125°g) and in agreement with the results summarized in Fig. 9. The S_2 ray path is steeper (by 8%) than the M_2 ray path and larger (~180°) phase changes occur for the S_2 component at this depth, perhaps indicating a more complete reflection for the S_2 tide at this position. The age of the internal tidal displacement at a depth of 3 and 62 km from the generating region is nearly 3 days after maximum barotropic tidal streaming at the shelf break. At distances greater than 62 km from the slopes, where the M_2 tide has more fully reflected from the sea floor, the age of the internal tide would be expected to decrease again near the main beam.

5. Conclusions and summary

Mowbray and Rarity (1967) demonstrated beams of internal wave energy propagating along characteristic paths emanating from an oscillating source in a laboratory experiment (see also Turner 1973). Pingree and New (1989) indicated that in the ocean the beam of internal tidal energy is likely to be very broad. The results presented here from the Bay of Biscay show that, at about 50 km from the upper slopes, in a water depth of 4 km, where the beam is at a depth of 3 km, the oscillations are essentially spread over the lower half of the water column. However, despite the broadness of the beam, it was still possible to follow the maximum oscillation amplitudes in the water column along a characteristic ray path. The CTD and thermistor chain observations presented in this paper, and summarized in Fig. 9, are believed to be the first reported field evidence demonstrating the propagation of a beam of internal tidal energy along a characteristic ray path from an identified source on the upper slopes to the point where the beam reflects off the ocean floor.

Phases along the beam, before reflection, were relatively constant, with an upward maximum displacement occurring at about 3 hours before HWP and an advance of phase with increasing depth. The upper-slope current moorings allowed an analysis for the M_2 tidal component. The results showed that the maximum upward displacement along the beam occurred about half an hour after the time of maximum upslope M_2 barotropic tidal streaming in the generating region, which determines the phase of the forcing term for the M_2 internal tide. The age of the internal tide near the shelf break was found to be only a few hours after barotropic spring tides. At mooring 116, in a water depth of 4202 m at 62 km from the critical slopes, a marked increase of M_2 internal tide phase (4½ hours) was observed at a depth of 3 km, where the maximum isotherm displacement occurred. At this depth the age of the internal tidal displacement was 3 days. Also at this position, the phase increased with depth in the 2 km

to 3 km depth range, and the M_2 currents were relatively large ($\sim$10 cm s^{-1}) near the sea floor. These facts are consistent with the upward propagation and partial reflection of internal tidal waves, as has been demonstrated by the comparison with the numerical model. The calculated M_2 ray path confirmed that the position of mooring 116 was just oceanward of the point of bottom reflection for a beam of internal tidal energy emanating from the critical point on the upper slopes in the Bay of Biscay.

It is interesting to speculate that moorings farther from the critical slope region than mooring 116 might show an upward propagating beam with the full +6.2 hour phase change, as predicted by the numerical model, and this will be the subject of further research. However, we believe that the present observations, which extend the results of PN farther out from the generation region, and are reinforced by the model, provide the first direct evidence for deep abyssal penetration and bottom reflection of internal tidal energy in nature.

Acknowledgments. Mooring 116 was designed, deployed and recovered by Ian Waddington. We also thank Bill Miller and the NERC Research Vessel Services Computing Group for assistance at sea. Part of this work has been carried out with the support of the Procurement Executive, Ministry of Defence.

REFERENCES

Baines, P. G., 1982: On internal tide generation models. *Deep-Sea Res.*, **29,** 307–338.

Barbee, W. B., J. G. Dworski, J. D. Irish, L. H. Larsen and M. Rattray Jr., 1985: Measurement of internal waves of tidal frequency near a continental boundary. *J. Geophys. Res.*, **80,** 1965–1974.

Gordon, R. L., 1979: Tidal interactions in a region of large bottom slope near northwest Africa during JOINT-1. *Deep-Sea Res.*, **26,** 199–210.

Huthnance, J. M., 1981: Waves and currents near the continental shelf edge. *Progress in Oceanography,* Vol. 10, Pergamon 193–226.

Larsen, L. H., M. Rattray Jr., W. B. Barbee and J. G. Dworski, 1972: Internal tides. *Rapp. P-V Réun.*, **162,** 65–79.

Le Cann, B., 1990: Barotropic tidal dynamics of the Bay of Biscay shelf. *Contin. Shelf Res.*, **10,**

Mowbray, D. E., and B. S. H. Rarity, 1967: A theoretical and experimental investigation of the phase configuration of internal waves of small amplitude in a density stratified liquid. *J. Fluid Mech.*, **28,** 1–16.

New, A. L., 1987: Internal tidal currents in the Bay of Biscay. *Advances in Underwater Technology, Ocean Science* and *Offshore Engineering,* Vol. 12, Graham and Trotman, pp. 279–293.

——, 1988: Internal tidal mixing in the Bay of Biscay. *Deep-Sea Res.*, **35,** 691–709.

Pingree, R. D., and A. L. New, 1989: Downward propagation of internal tidal energy into the Bay of Biscay. *Deep-Sea Res.*, **36,** 735–758.

——, D. K. Griffiths and G. T. Mardell, 1984: The structure of the internal tide at the Celtic Sea shelf break. *J. Mar. Biol. Assoc. U.K.*, **64,** 99–113.

——, G. T. Mardell and A. L. New, 1986: Propagation of internal tides from the upper slopes of the Bay of Biscay. *Nature,* **321,** 154–158.

Prinsenberg, S. J., and M. Rattray, 1975: Effects of continental slope and variable Brunt-Väisälä frequency on the coastal generation of internal tides. *Deep-Sea Res.*, **22,** 251–263.

Schott, F., 1977: On the energetics of baroclinic tides in the North Atlantic. *Ann. Géophys.*, **33,** 41–62.

Turner, J. S., 1973: *Buoyancy Effects in Fluids.* Cambridge University Press, 368 pp.